Raman studies of hexagonal ZnS:Al

A. Król,* A. Hoffmann, and J. Gutowski
Institute für Festkörperphysik, Technische Universität Berlin, Hardenbergstrasse 36, D-1000 Berlin 12, Germany
(Received 3 March 1988)

Raman spectra of ZnS heavily doped with Al in the Stokes region of 400 to 500 cm^{-1} show several distinct lines on the low-energy side of hexagonal-host modes. They are independent of temperature and thus attributed to Al-related local phonons. From vibrational-mode analysis and by comparison with ir data we can assign the lines to isolated Al_{Zn}, Al_{Zn}-V_{Zn} next-nearest-neighbor pairs, Al_{Zn}-Cu_{Zn} donor-acceptor pairs, and other Al-related point defects (where V_{Zn} denotes a Zn vacancy).

Although ZnS:Al is a very important phosphor, our knowledge of Al-related defects is still not complete. In previous papers we reported on the influence of Al as a dopant on the crystal structure of ZnS (Ref. 1) and on the infrared (ir) absorption data in ZnS:Al.[2] The phase transition from cubic ($3C$) to the hexagonal ($2H$) modification of ZnS with increasing Al concentration was established. It was shown that Al_{Zn}-V_{Zn} next-nearest-neighbor pairs (where V_{Zn} denotes a zinc vacancy) play an important role in the structural transition[1] and luminescence.[3]

The purpose of the present work is the investigation of local phonons in hexagonal ($2H$) ZnS:Al crystals by means of Raman spectroscopy.

The investigated ZnS:Al crystals were obtained by the high-pressure Bridgman method at Warsaw Technical University. The Al concentration exceeds 10^{19} atoms cm^{-3}. The crystal structure was examined by x-ray diffraction and all studied samples were found to be pure $2H$ polytypes (wurtzite structure).

The Raman spectra were obtained with a Spex Industries double-grating monochromator and a double-prism premonochromator at 1.5 K and room temperature (RT). The resolution of the apparatus was restricted to about 3 cm^{-1} due to strong luminescence background.

All investigated crystals exhibited strong luminescence with a maximum at 560 nm which is very similar to results obtained by Hoshina and Kawai.[3] On the one hand, this hindered our experiment and resulted in a considerable lowering of spectral resolution. On the other hand, it became clear from photoluminescence and excitation spectra that Al-related centers contribute dominantly to the feature of the spectra. The characteristic blue luminescence observed at 430 nm has been attributed to Al-Cu donor-acceptor recombination.[4] Efficient excitation was possible, which demonstrates a pronounced energy transfer to these impurities. For lower energies, the decrease of excitability sets in when the laser energy falls short of the pair transition energy.

A typical Raman spectrum of an Al-doped ZnS crystal at RT is given in Fig. 1 for a right-angle scattering configuration. All spectra are labeled with four letters [here $x(z,x)y$]. These letters refer to the laboratory coordinate system. The first and last letters are the directions of propagation of the incident and scattered light, respectively, and the middle two letters in parenthesis give the polarization of the incident and scattered light, respectively. The crystallographic c axis is along the z laboratory coordinate (with 5° accuracy in our experiment). The comparison of the obtained Raman spectra in different scattering configurations with previously published data confirms that ZnS crystals doped with Al in a concentration exceeding 10^{19} atoms cm^{-3} have strong hexagonal modifications, since the observed Raman modes are rather typical for wurtzite ($2H$) ZnS. They are presented in Table I and are in a good agreement with the Raman[5] and infrared[6] data.

According to our ir studies[2] no Al-related localized phonons are expected in the spectral range below 400 cm^{-1}. In this regime all scattering lines can be explained in terms of a Raman effect on lattice phonons. Our measurements confirmed strong dependence on temperature of Raman modes in this spectral region.

In the regime between 400 and 500 cm^{-1} one should not only expect the existence of lattice-phonon combinations, but also of local modes representing Al-related point-defect vibrations. For this reason we investigated this spectral region at 1.5 K and RT for $x(z,z)y$ and $x(z,x)y$ configurations at two laser wavelengths (488.0-

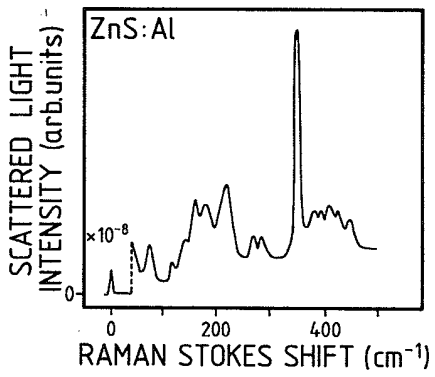

FIG. 1. Raman spectrum of the $2H$-ZnS:Al crystal ([Al]$=4.2\times10^{19}$ atoms cm^{-3}), excited with the 488.0-nm line of an Ar laser at room temperature in x(z,unpolarized)y configuration.

TABLE I. Host modes of 2*H*-ZnS:Al at 300 K in cm^{-1}.

Mode	Energy shift this work	Energy shift Ref. 5	ir data Ref. 6
LO(E_1)	351	347.8	346
TO(E_2)	281	283	297
TO(E_1)	274	273	
TO(A_1)	271	267	
LA	178		181
TA(E_2)	71	69.2	70
TA(E_1)	56	56.2[a]	

[a]Obtained for ZnS 4*H* polytype.

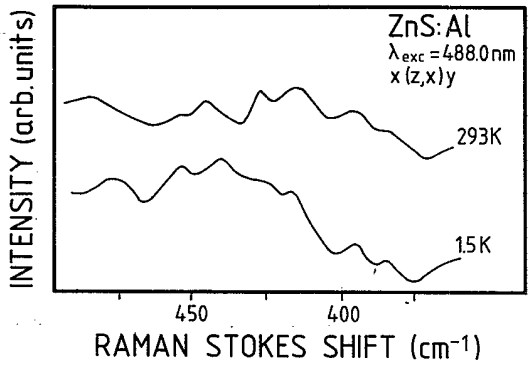

FIG. 3. As Fig. 2, but for $x(z,x)y$ scattering geometry.

and 514.5-nm lines of the Ar-ion laser). The results obtained for 488.0-nm excitation are shown in Figs. 2 and 3, respectively. The dominant Raman lines in this regime are independent of temperature, in contrast to the lattice-phonon combinations, e.g., those at 158, 178, or 220 cm^{-1}. Thus, we conclude that they must be due to local modes. Table II contains all observed Raman lines in the spectral region 400–500 cm^{-1} on the low-energy side of the laser for 488.0 nm as well as for a 514.5-nm excitation at 1.5 K. They are contrasted with the ir data.[2,7] Due to the strong blue luminescence some Raman modes are not visible under excitation with the blue laser line.

The symmetry of the localized vibrational modes (LVM's) was studied by analyzing the polarization of the scattered light. The central Raman lines at approximately 440 cm^{-1} can be assigned to the localized vibration of an unassociated aluminum impurity at the zinc site. This mode of vibration has F_2 symmetry in the T_d point group. Due to the hexagonal crystallization of the samples the point-group symmetry is now reduced from T_d to C_{3v}. Thus, the energy level of the localized oscillator in T_d splits into two energy levels in C_{3v}, one with A_1 and the other with E symmetry. The A_1 mode observed in $x(z,z)y$ scattering geometry has an energy of 429 cm^{-1}, whereas the E mode in $x(z,x)y$ is situated at 440 cm^{-1}, which is in good agreement with the ir data (see Table II).

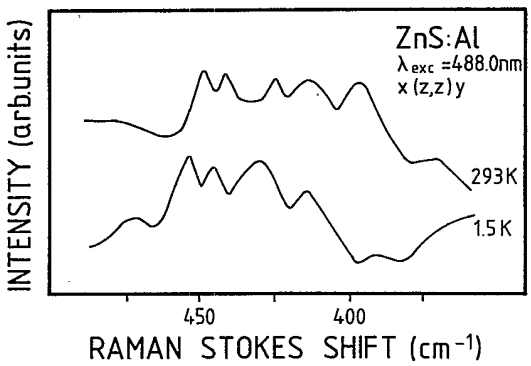

FIG. 2. Raman spectrum of 2*H*-ZnS:Al in the region of Al-related localized modes of vibrations for two different temperatures and $x(z,z)y$ scattering geometry, excited with the 488.0-nm laser line of an Ar laser ([Al]$=4.2\times10^{19}$ atoms cm^{-3}).

The incorporation of aluminum into the substitional zinc site in the ZnS lattice induces donor-acceptor pair formation, with a Al_{Zn}-V_{Zn} complex-type dominant defect.[7] In a crystal with the hexagonal 2*H* structure two types of next-nearest-neighbor pairs can be distinguished: a pair with its axis perpendicular or at an acute angle with the crystallographic c axis, with C_1 or C_S site symmetry, respectively. LVM's of such oscillators can be divided into stretching mode [$A(3)$ in C_1, or, $A'(1)$ in C_S], bending mode in the plane of the axis of the pair and crystallographic c axis [$A(2)$ or $A'(2)$], and bending mode perpendicular to this plane [$A(3)$ or A'']. From vibrational-mode analysis all these modes are found to be Raman active. With regard to our configurations measured, $A'(1)$ and $A'(2)$ LVM's can be observed only in the $x(z,z)y$ scattering geometry while A'' can appear only in the $x(z,x)y$ configuration. This limitation does not apply to Raman lines due to LVM's of C_1-type complexes. From vibrational-mode analysis it follows also that the stretching localized mode of the pair should have higher frequency than the LVM created by an unassociated impurity. In turn, the bending LVM of the pair are expected to have lower energies than the isolated impurity. For a weakly coupled pair, one can also expect that frequencies of paired localized vibrations fulfill the frequency-sum rule and center on the LVM of an unassociated impurity.[2] Taking all these results into account we can identify the Raman line at 472 cm^{-1}, which is observed only in the $x(z,z)y$ scattering geometry (see Fig. 2), as originating from a localized stretching mode with $A'(1)$ symmetry. In the same manner we ascribe localized bending mode with A'' symmetry to the Raman line which appears at 425 cm^{-1} in the $x(z,x)y$ configuration only (see Fig. 3). From the frequency-sum rule we predict that the second bending mode of the C_S-type pair, with $A'(2)$ symmetry, should be located at about 420 cm^{-1}. However, due to appearance of a very broad band with a maximum at 429(426) cm^{-1} in the Raman spectrum, obtained for $x(z,x)y$ scattering geometry and with the low resolution of our apparatus, the $A'(2)$ Raman line cannot be resolved in our experiment.

TABLE II. Raman modes in 2*H*-ZnS:Al in the regime 400–500 cm^{-1} for 488.0- and 514.5-nm excitation compared with ir data obtained for 2*H*-ZnS:Al (Ref. 2) and 3*C*-ZnS:AL,Cu (Ref. 7). *A* and *B* denotes Al_{Zn}-V_{Zn} next-nearest-neighbor pairs with C_1 and C_s symmetry, respectively. *C*, *D*, and *E* denote isolated Al_{Zn},Al_{Zn}-Cu_{Zn} donor-acceptor pairs, and unknown Al-related point defects, respectively.

	Raman lines at 1.5 K in cm^{-1}				ir modes at 80 K in cm^{-1}		
Proposed	λ_{exc}=488.0 nm		λ_{exc}=514.5 nm		3*C* (Ref. 7)	2*H* (Ref. 2)	ZnS:Al
defect	$x(z,z)y$	$x(z,x)y$	$x(z,z)y$	$x(z,x)y$	ZnS:Al,Cu	E$\|\|\hat{c}$	E$\perp\hat{c}$
A	412		414			411.5	
A		416				420	420.5
B,*D*		425[a]		423	422.5		423
B,*C*,*D*	429[a]		426		428		
C		440				432	438
E	444		447	444		444	445
D,*E*	455	454			460	450	458
B	472					477	
A		477					481.5

[a]Unresolved broad band.

The low-frequency Raman lines around 414 cm^{-1} observed in both experimental configurations are attributed to localized bending mode with $A(2)$ symmetry. The high-frequency Raman line at 477 cm^{-1} at the $x(z,x)y$ scattering geometry is due to an $A(3)$ stretching LVM. This line is also expected to be observed at $x(z,z)y$ geometry. However, it is not resolved in our experiment, most likely due to poor resolution. The remaining low-frequency $A(1)$ bending LVM is hidden under the wings of broad Raman lines at 429(426) and 425(423) cm^{-1} at $x(z,z)y$ and $x(z,x)y$ scattering geometries, respectively.

The Raman line at 455 cm^{-1} observed at both experimental configurations can be attributed to the stretching LVM of an Al_{Zn}-Cu_{Zn} donor-acceptor pair. Existence of such pairs in the investigated crystals was revealed in our photoluminescence studies. The low-frequency bending LVM's are expected in the spectral regime around 425 cm^{-1} and cannot be resolved in our experiment. The Raman lines at 444 cm^{-1} are due to unknown Al-related defects.[8]

A comparison of our Raman data with ir results provides us with independent verification of the attribution of the Raman lines proposed in this work. We would like to note a very good agreement of experimental results obtained by Raman scattering and ir absorption collected in Table II.

In summary, we report on the Raman study of ZnS heavily doped with Al, and therefore with pure wurtzite structure. The features observed in the Raman spectra can be divided into two classes.

(1) Raman lines stemming from two-phonon processes being typical for the hexagonal (2*H*) modification of ZnS.

(2) Raman lines due to scattering at localized phonons originating from the Al_{Zn} isolated impurity, Al_{Zn}-V_{Zn} next-nearest-neighbor pairs, Al_{Zn}-Cu_{Zn} donor-acceptor pairs or some other unknown Al-related point defects. As is fully consistent with the ir data, we conclude that the above-mentioned defects thus dominate in the investigated systems.

ACKNOWLEDGMENTS

We are grateful to M. Jasionek and M. J. Kozielski for providing us with the ZnS:Al crystals and x-ray tests.

*Also at Institute of Experimental Physics, Warsaw University, ul. Hoza 69, PL-00-681 Warszawa, Poland. Present address: Department of Physics, State University of New York at Stony Brook, Stony Brook, NY 11794-3800.

[1]A. Król, M. J. Kozielski, and W. Nazarewicz, Bull. Minéral. (France) **109**, 81 (1986).

[2]A. Król and W. Nazarewicz, J. Phys. C **18**, 467 (1985).

[3]T. Hoshina and H. Kawai, Jpn. J. Appl. Phys. **19**, 267 (1980).

[4]V. Gool, A. P. Cleiren, and H. J. M. Heijligers, Philips Res. Rep. **15**, 254 (1960).

[5]J. Schneider and R. P. Kirby, Phys. Rev. B **6**, 1290 (1972).

[6]R. Marshall and S. S. Mitra, Phys. Rev. **134**, A1019 (1964).

[7]A. Król, M. J. Kozielski, and W. Nazarewicz, Phys. Status Solidi B **90**, 649 (1978).

[8]W. M. Theis, D. N. Talwar, M. Vandevyver, and W. G. Spitzer, J. Appl. Phys. **58**, 2553 (1985).